Proceedings World Geothermal Congress 2020+1
Reykjavik, Iceland, April - October 2021

The Thermal Structure of the Upper Crust in Central-Southern Italy and its Correlation with the Distribution of Geothermal Resources

Gianluca Gola[1*], Serena Botteghi[1], Francesco Brozzetti[2], Claudio Chiarabba[3], Rita De Nardis[2], Federica Ferrarini[2], Gianluca Groppelli[4], Giusy Lavecchia[2], Pier Paolo Limoni[5], Domenico Montanari[6], Gianluca Norini[4], Lorenzo Petracchini[7], Maurizio Polemio[5], Francesca Santaloia[5], Alessandro Santilano[1], Davide Scrocca[7], Eugenio Trumpy[1] and Adele Manzella[1]

1-Institute of Geosciences and Earth resources (IGG-CNR), National Research Council, Pisa, Italy; 2-Earth Science Department, University of Chieti, Chieti, Italy; 3-Istituto Nazionale di Geofisica e Vulcanologia (INGV), Rome, Italy; 4- Institute of Environmental Geology and Geoengineering (IGAG-CNR), National Research Council, Milan, Italy; 5-Institute for Geo-hydrological Protection (IRPI-CNR), National Research Council, Bari, Italy; 6-Institute of Geosciences and Earth resources (IGG-CNR), National Research Council, Florence, Italy;7-Institute of Environmental Geology and Geoengineering (IGAG-CNR), National Research Council, Rome, Italy

[*]gianluca.gola@igg.cnr.it

Keywords: Thermal Modelling, Geothermal Resources, Central-Southern Italy

ABSTRACT

Temperature is a key parameter in controlling the *in-situ* petrophysical properties, the solid and fluid phase equilibria, the stress-strain relationships as well as the occurrence and potential of geothermal resources. Thermal field anomalies are determined by a great number of different factors and the study of their nature together with a quantitative appraisal are critical in mapping the spatial distribution of the conventional and unconventional geothermal resources as well as estimating the deep crustal conditions and their lateral variability. With the aim to study the thermal structure of the upper crustal levels in Central-Southern Italy, we exploited lithostratigraphic, hydrological, petrophysical and geophysical data. We described the main heat transport phenomena occurring in the upper crust and we applied these concepts to a numerical modelling approach. We developed a new 3D geological model considering the main lithothermal units acting as the cap-rock of the deep-seated hydrothermal systems, the regional carbonate reservoirs and the crystalline/metamorphic basement. The temperature data from the accessible deep boreholes represented the main thermal constraints of the models. The maximum logged depth is about 7 km, although the majority of the data distributes in the depth range 1.5-3.5 km. At greater depths, seismological and rheological evidence (i.e. the thickness of the seismogenic layer) gave us further indirect information regarding the deep thermal state of the upper crust. Along the Apennine chain, particularly in correspondence of outcropping carbonate units, the temperature distribution is affected by downward heat advection. The most favourable geological conditions leading to the development of high temperature hydrothermal systems occur far from the outcropping carbonate units; especially in the Tyrrhenian side of the peninsula affected by crustal stretching and Plio-Pleistocene magmatic activity.

1. INTRODUCTION

Thermal conduction and hydrothermal convection are the two main heat transport mechanisms controlling the thermal structure of the solid Earth. Geothermal and metamorphic studies provided indications that conductive heat transfer dominates in the middle-to-lower continental crust where the permeability of the crystalline/metamorphic basement, typically in the range of 10^{-20} m^2 to 10^{-16} m^2, limits an efficient convective heat transport (Ingebrigtsen and Manning 2003, Manning and Ingebrigtsen 1999). Nevertheless, in many tectonically active areas anomalously high geothermal gradients have been measured at shallow depths (Cloetingh et al. 2010, Ranalli and Rybach 2005). In these environments, downward extrapolation of the geotherm assuming a purely conductive regime could lead to extremely high, even unrealistic, temperatures in the deeper levels. Assumptions of a non-negligible convective heat transport, controlled by fluid movement in the permeable rocks, and even the occurrence of upper-middle crustal heat sources of magmatic origin might provide a reasonable solution to this problem.

In Central-Southern Italy, the pronounced lateral variability of the observed terrestrial heat flow (Della Vedova et al. 2000, Mongelli et al. 1991) reflects its complex structural setting and the coexistence of conductive-convective heat transport phenomena. Since the permeability of the shallow crustal levels in the area of study are mainly dominated by the carbonate platform units whose permeability can exceeds locally the threshold value for a well-organized hydrothermal convection (~10^{-14} – 10^{-13} m^2), the magnitude of the convective heat flow component can be greater than the conductive one by many times. Where the favourable geological conditions lead to the development of a deep-seated hydrothermal systems, the thermal energy transported by upwelling fluids is responsible of the observed anomalously high heat flow values greater than 10^2 mW/m^2. Conversely, in proximity of the Apennine chain, downward fluid flow from the recharge areas is responsible for the deepening of isotherms resulting in an apparent low heat flow (30-40 mW/m^2).

This work falls within the Geothermal Atlas Project aimed at characterizing, assessing and mapping of conventional and unconventional geothermal resources for power production in Central-Southern Italy. In order to infer the temperature distribution in the upper crustal levels and characterising the distribution of geothermal resources, we exploited a multidisciplinary dataset, i.e. lithostratigraphic, hydrological, petrophysical and geophysical information. We numerically simulated the main heat transport processes occurring in the upper crust tacking into account the coupled conductive-convective heat transfert in porous media and the temperature dependence of the physical properties of the fluid-rock system. The results of the numerical models were then compared with a large set of deep borehole temperatures enabling the calibration of the assumed boundary conditions.

2. GEOLOGICAL SETTING

The geological and structural setting of Central-Southern Italy is characterized by the presence of a complex arcuate thrust belt system belonging to the peri-Mediterranean orogenic belt which was generated by the relative movements between the Eurasian and African plates and by the interactions with the Adriatic microplate (e.g. Faccenna et al. 2004, Doglioni et al. 1999, Dewey et al. 1989, Malinverno and Ryan 1986). The peri-Mediterranean orogenic belt is made up by three main segments (i.e. the Central-Southern Apennines, the Calabrian Arc, and the Sicilian Maghrebides) and each one is associated with its foredeep and foreland domains, while the common internal sector is marked by the Tyrrhenian Sea (Figure 1). Although several geodynamic interpretations have been proposed to explain the development of this orogenic belt (e.g. Lavecchia et al. 2003, Liotta et al. 1998, Doglioni 1991, Royden et al. 1987, Scandone 1980), it is generally agreed that the three above-mentioned orogenic segments reflect the original heterogeneities of the Mesozoic paleogeographic domains that were deformed during the growth of the thrust belt system.

The original Meso-Cenozoic sedimentary covers deposited on the Ionian oceanic basin and on the two conjugate Apulo-Adriatic and African passive margins were off-scraped and incorporated respectively in the Calabrian Arc, Central-Southern Apennines and Sicilian Maghrebides. These sedimentary covers are mainly made up of evaporites, shallow water and pelagic carbonates in the case of the two passive margins, and by deeper water terrigenous units and ophiolite bearing sequences in the case of the Ionian basin. Since Oligocene, the presence of both foredeep and piggy-back basins progressively younger towards the foreland clearly document the migration of the thrust belt front (e.g. Patacca and Scandone 2004 and 1990, Boccaletti et al. 1990). From Middle-Late Miocene, the progressive foreland-ward migration of the accretionary prism was accompanied by crustal stretching of the internal sectors of the belt, controlling the genesis of the Tyrrhenian Sea (Scrocca et al. 2012, Malinverno and Ryan 1986). In this context, metamorphic basement slices outcropping in the Kabilo-Calabride and Peloritani sectors (Calabrian Arc and north-eastern Sicily) may be considered relics of the stretched and boudinated Alpine belt (Carminati et al. 2004).

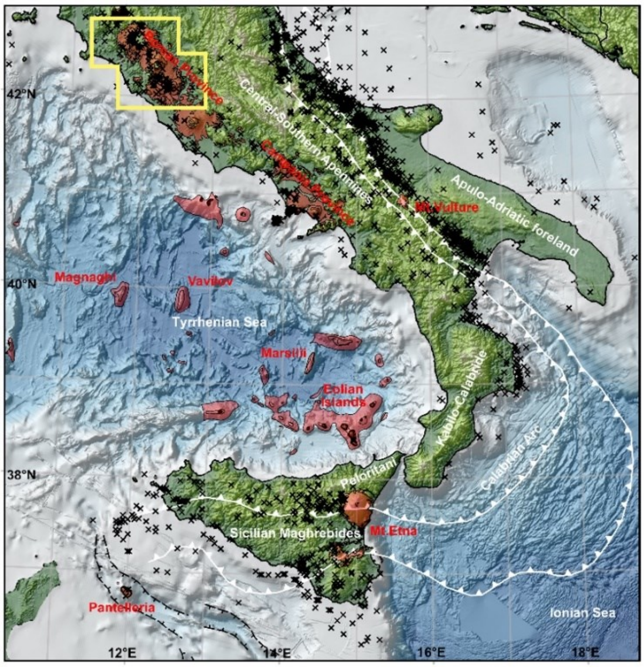

Figure 1: Geological and structural setting of the area of study. In the map, the exploited boreholes (cross symbols), the internal and external Apennine thrust fronts (white lines), the Pliocene-Pleistocene volcanic centers (red areas) and the extension of the numerical model (yellow polygon) of Figure 4 are reported.

The complexity of the Tyrrhenian-Apennines system is also expressed by the large variety of the Plio-Quaternary volcanic rocks erupted in the study area. The magmatism occurs along a NW-SE trending extensional zone on the Tyrrhenian side of the Italian peninsula (Roman Province, Campania Province and Mt.Vulture), in eastern Sicily (Mt.Etna), on the Tyrrhenian sea floor (Eolian Islands, Magnaghi-Vavilov and Marsilii seamounts) and in the Sicily Rift Channel (Pantelleria Island). From a geodynamical point of view, few different associations may be distinguished. The calcalkaline-shoshonitic series of the Roman Province, Campania Province and Eolian Islands are related to the subduction of the Adriatic continental lithosphere and Ionian oceanic lithosphere. The alkaline-tholeiitic associations in the Magnaghi-Vavilov and Marsilii seamounts are instead related to the back-arc extension of the Tyrrhenian Sea. To explain the intermediate signatures from OIB-type and arc-type of the mafic rocks from the Campania Province and Mt.Vulture, an input of asthenospheric mantle from the Apulia foreland and contemporaneous contamination by sedimentary material and fluids coming from the Ionian slab were invoked. The migration of asthenospheric material from Apulia to the Campania region was favoured by the opening of a slab window generated by the slab break-off of the Apulian plate (Peccerillo 2005). According to this recent view, the faster rollback of the Ionian plate with respect to the African plate controlled the melting of a hybrid mantle feeding the Mt.Etna volcanism. The Island of Pantelleria shows many characteristics that are commonly found in volcanoes from continental rift settings.

3. EXPLORATION DATA

In order to constrain the deep-sated geological structures and the underground temperature distribution, we exploited litho-stratigraphic, geophysical and drill-stem test (DST) data from about 1000 boreholes in the study area and from the Italian National Geothermal Database platform managed by the National Research Council of Italy (Trumpy and Manzella 2017). Specific queries where then prepared to extract the datasets needed for: i) the 3D geological model, ii) the 3D thermal model, iii) the definition of the petrophysical properties and iv) the characterization of the regional flow paths.

3.1 Thermal data

Reliable subsurface temperatures are essential in geothermal studies. The dataset we exploited consists of borehole temperatures measured down to a maximum depth of about 7 km, although most of the data ranges between 1-3 km (see Figure 1 for the borehole distribution). Geothermal boreholes provided static bottom-hole temperatures measured after large shut-in times (i.e. the time elapsed since the end of the circulation of the drilling mud to the temperature measurement variable from several days to some months). In the thrust belt and foredeep areas, hydrocarbon exploratory wells provided a huge set of data; essentially raw bottom-hole temperatures (BHT). The analysed BHTs have short shut-in times ranging from 2 to 60 hours with an average value of about 10 hours. As these times are too short to permit a full thermal recovery of the borehole after the drilling operations, the raw BHTs systematically underestimated the real formation temperature (Deming 1989). To correct the raw BHTs, we applied two different techniques depending on the available data and their characteristic. For more than 250 time-temperature series we applied the well-known Horner procedure (Dowdle & Cobb 1975, Horner 1951). When only one BHT was available, we calibrated with our dataset an empirical correction method based on the correlation between the Horner slope and the depth (Pasquale et al. 2008). The best-fitting curve of the Horner slope data through the measurement depth is shown in Figure 2. We checked the accuracy of the latter correction procedure by the comparison of the time-temperature series corrected by the Horner method, which were taken as reference values, with the same raw data corrected individually as a single BHT by the empirical equation. As shown in Figure 2, the relative differences decrease as the shut-in time increases. The empirical correction statistically does not over-estimate or under-estimate the real formation temperature in comparison with the Horner method. Nevertheless, in the case of single BHTs, due to the intrinsically low quality of the measurement (±2°C) and shut-in times that usually do not exceed 10-20 hours, we may assume an average error in the corrected temperatures of ±10%.

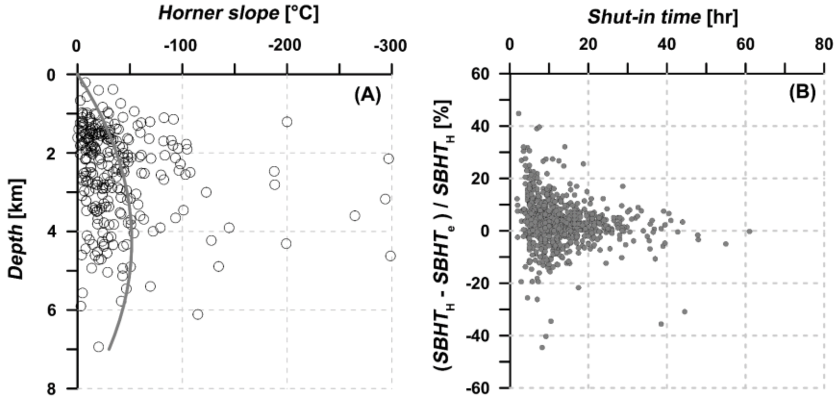

Figure 2: Calibration and validation of the empirical BHT correction. (A) Horner-slope data as function of the measurement depth of the time-temperature series together with the 2nd-order polynomial fitting curve. (B) Relative differences between the time-temperature series corrected by the Horner method ($SBHT_H$) and the same temperatures corrected individually by the empirical formula ($SBHT_e$) as function of the shut-in time.

3.2 DST data

From the static fluid pressures measured and/or extrapolated during DST tests we evaluated the potentiometric head in order to obtain a spatial parameter able to describe the regional flow paths. The DSTs involving only water as liquid monophasic fluid were selected which improved accuracy and simplified data processing. Therefore, 290 DSTs, performed in 180 wells and located between +330 and -4500 m a.s.l., were chosen. 100 DSTs involved the carbonate reservoir while the remaining 190 were carried out in the overlying sedimentary sequences. Fluid density values from DST reports and the dependence of fluid density upon temperature were considered in the computation. If more than one test was available for a single well, the vertical direction of the potentiometric gradient has been also determined. In particular, the vertical direction was found to be oriented downward moving inland (far away from the coastlines) while an upward gradient was mostly measured approaching the coastal areas. This pattern is more evident in the case of sedimentary sequences overlying the carbonate reservoir. This seems the effect of inland prevalent recharging flow due to leakage from overlying aquifer formations. On the contrary, close to the coast, the boundary effect of the sea could justify the prevalent upward flow direction. Apart from Sicily, groundwater flow in the sedimentary successions is clearly divergent from inner areas; this corresponds to the highest altitudes of the southern Apennines towards the coasts. The groundwater flow of Sicily is divergent from the reliefs arranged along an N-S axis and is placed in a central position of the island. Apart from Sicily, the outcropping carbonate morphological highs shows to influence the groundwater flows in the deep-seated carbonate reservoir. The flow diverges from the carbonate morphological highs and converges towards the top reservoir lows. In Sicily, the flow diverges from the central portion of the island mainly toward the southern coast along two directions (NNE-SSW and NW-SE).

3.3 Top and bottom of the regional carbonate reservoir

By merging regional hydrogeological information and borehole data, the regional aquifer matched to the Meso-Cenozoic carbonate units (Montanari et al. 2017 and 2014, ENEL/ENI–AGIP/CNR/ENEA 1988 and 1994). Although both lateral and vertical anisotropies occur, these units are made up by Upper Triassic-Middle Miocene shallow water carbonates, transitional shelf-to-basin deposits, and pelagic sequences. It should be noted that, due the aforementioned structural and stratigraphic complexities, in the different geological domains the surface that identifies the top of the carbonate units representing the regional geothermal reservoir corresponds to different geological formations. Taking into consideration the above described stratigraphic and structural setting, to generate 3D surfaces useful for the thermal modelling exercise the top of regional geothermal aquifer has been built merging along the axial part of the chain the top of carbonate units flexured below the foredeep deposits with the top of carbonate units recognisable in outcrop or at shallow depth along the internal side of the thrust belt. The resulting surface is displayed in Figure 3. The lower boundary of the regional carbonate reservoir has been rough out by the top of the crystalline/metamorphic basement, as defined from geophysical data in Cassano et al. (1986) and Montanari et al. (2017).

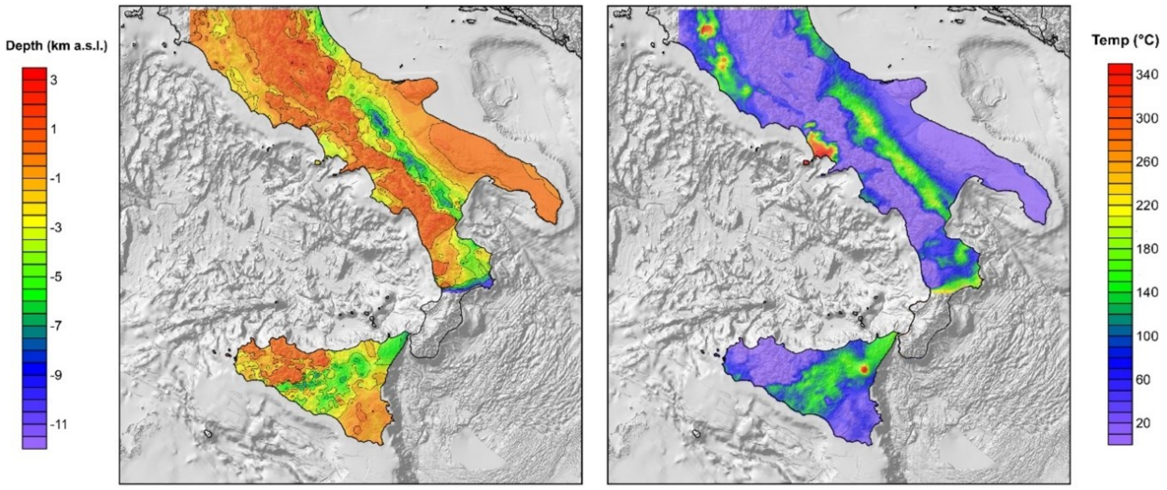

Figure 3: Depth (in km a.s.l.) to the top of the modelled regional carbonate reservoir (left) and temperature distribution (in °C) at the top of the regional carbonate reservoir resulting from the calibrated numerical models (right).

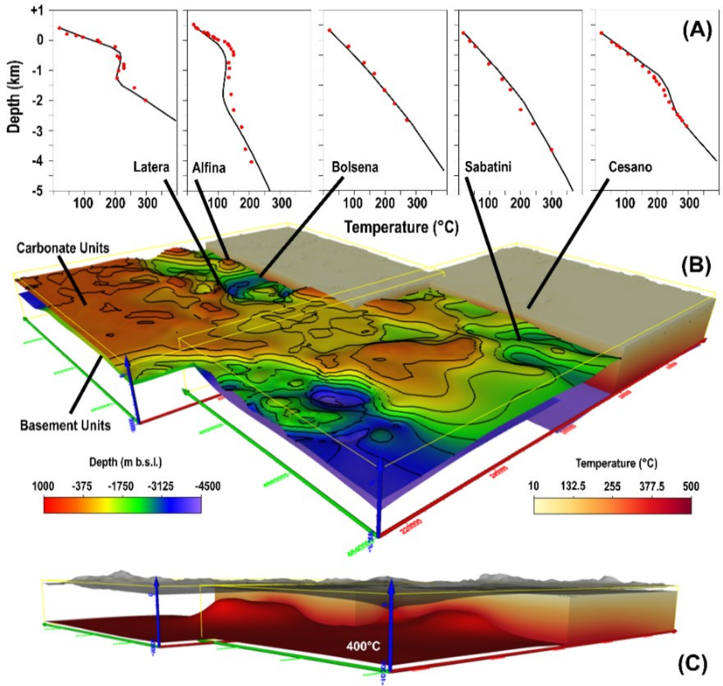

Figure 4: 3D thermal model of the Northern Latium sector (see Figure 1 for the extension of the numerical domain). (A) The comparison between the simulated (black line) and measured (red circles) temperatures in selected deep boreholes, (B) the top of the carbonate and basement units and (C) the modulation in depth of the 400°C isotherm are shown.

4. THERMAL MODELS

To study the steady-state thermal structure resulting from the coupled heat transfer and fluid flow equations, we set-up several numerical models. Each of them was characterized by a computational domain of about 100x100x15 km^3. The geological model previously defined consists of three main surfaces, from the top to the bottom: i) the topography and/or bathymetry, ii) the top of the carbonate units hosting the regional hydrothermal reservoir and iii) the top of the crystalline/metamorphic basement. The geothermal system is described by the combination of the continuity and momentum equations; together they form the Brinkman equations and the heat transport equation. In the case of stationary, incompressible flow, the mass continuity equation simplifies to a volume continuity equation:

$$\nabla \mathbf{u} = 0 \qquad (1)$$

where **u** is the fluid velocity vector (m/s). The momentum conservation is:

$$\nabla P = -\frac{\mu_w}{K}\mathbf{u} + \frac{\mu_w}{\phi}\nabla^2\mathbf{u} + \mathbf{F} \quad (2)$$

where P is the pressure (Pa), ϕ the porosity, μ_w the fluid dynamic viscosity (Pa s), K the permeability of the porous rock (m^2) and **F** is the volume force term (kg m^{-2} s^{-2}). As can be seen in equation 2, there are two viscous terms. The first is identified as the Darcy's term and the second is a Laplacian term that is normally included in the Navier-Stokes equation. By using this extension, the wall shear stress is accounted for in the momentum equation when the porous media is bounded by impermeable surfaces. Neglecting the boundary effects in the flow and heat transfer in a porous medium next to a solid boundary could lead to significant errors in heat transfer calculations. The term **F** in the momentum equation represents the gravity and buoyancy forces acting on the fluid. We further assume that the fluid phase and the solid phase are in local thermal equilibrium, and the heat generation due to viscous dissipation is negligible. Then, the energy conservation accounting for both solid matrix and fluid properties becomes:

$$k_b\nabla^2 T - \left(\rho c_P\right)_w \mathbf{u}\nabla T = A \quad (3)$$

where T is the temperature (K), k the thermal conductivity (W m^{-1} K^{-1}), ρ the density (kg m^{-3}), c_p the specific heat capacity at constant pressure (J kg^{-1} K^{-1})) and A the radiogenic heat production (μW m^{-3}). The subscripts b and w refer to the rock bulk and water properties, respectively.

Thermal petrophysics was investigated for porosity, thermal conductivity, radiogenic heat production and hydraulic permeability. The lithothermal units were treated as a homogeneous and downward anisotropic porous material (Pasquale et al. 2011). Mixing laws were applied to estimate the effective thermal properties of the rock-fluid system accounting for the *in situ* conditions (depth and temperature). In order to establish reliable porosity-depth and permeability-depth relationships and to infer accurate thermal conductivity and radiogenic heat production values by lithothermal unit, we integrated a large set of laboratory data, wire-line logs and DST pressure data. Moreover, from the master logs of about 100 hydrocarbon exploratory wells we collected a total of 800 porosity and 600 permeability data measured on 400 core plugs at Eni spa laboratories. A further compilation of water-saturated thermal conductivity measurements, comprehensive of X-ray diffraction and porosity information is used to assess the matrix thermal conductivity of the main lithothermal units. This approach allowed a consistent definition of input parameter for the thermal numerical models.

Since the rocks above the carbonate reservoir (i.e. the cap-rock units) and the crystalline/metamorphic basement are mainly constituted by impervious rocks (i.e. hydraulic permeability $K < 10^{-16}$ m^2), we evaluated the thermal effects of the interplay of the free convection and topographically driven groundwater flow in the permeable carbonate reservoir. Locally, we accounted for the thermal effects of crustal magmatic bodies of variable sizes, emplacement depths and temperatures. The magmatic intrusion is modelled by a hot domain constrained by volcanological and geophysical evidences with fixed surface temperature releasing heat in the surrounding rocks by conduction. The best-fitting solution is evaluated by solving a set of possible scenarios and computing the root-mean-square error (RMSE) between the simulated thermal profiles and the measured data in the boreholes. The calibration procedure enabled us to select the most suitable set of boundary conditions which minimizes the RMSEs. Further details on the numerical models can be found in Montanari et al. (2017) and Castaldo et al. (2017). As an example of the setting, calibration and output of the numerical models, the Figure 4 shows the 3D geological and thermal models of the Northern Latium sector (see Figure 1 for the areal extension of the numerical domain). The temperature distribution at the top of the regional carbonate reservoir is displayed in Figure 3. The most import thermal anomalies rely to the western side of the area of study and they are localized within the well-known volcanic area of Plio-Pleistocene age. Here, the temperature at the top of the regional reservoir is greater than 280-320°C. Outside the volcanic areas, other interesting hydrothermal anomalies occur within the carbonate reservoir far enough from recharge areas and characterized by temperatures in the range 150-180°C.

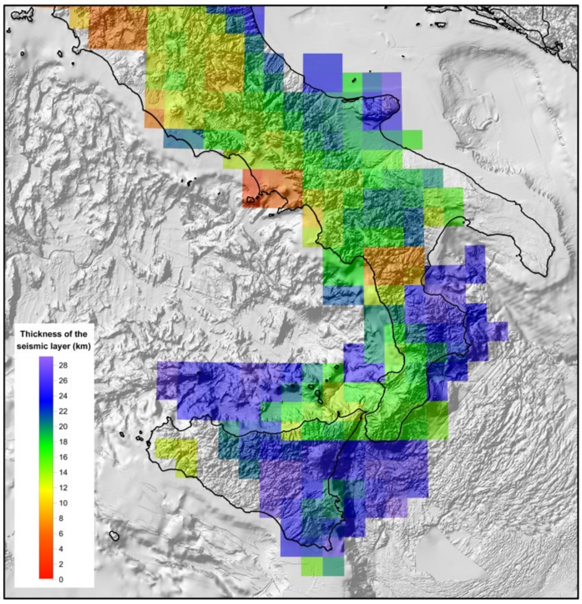

Figure 5: Thickness of the seismic layer in the Central-Southern Italy defined as the 90th percentile of the cumulative frequency-depth distribution of the crustal seismicity.

5. THICKNESS OF THE SEISMIC LAYER

The transition from brittle faulting to plastic flow depends on several factors such as temperature, rock composition and strain rate. In Italy the thermal control on the seismogenic thickness is well documented since the anomalously shallow cut-off depths of seismicity roughly mimic the heat flow anomalies (Chiarabba and De Gori 2016). In this study, we analysed the relocated earthquake catalogue (Chiarabba et al., 2015 and subsequent upgrades from INGV database) and evaluated the cut-off depth of crustal seismicity. The high density and quite uniform distribution of the earthquakes in the catalogue, having a completeness magnitude of about $M_L >$ 1.5, allowed a robust statistical analysis. Furthermore, only earthquakes with hypocentre errors of less than 1 km and rms lower than 0.8 s were selected. We determined a depth histogram for the seismicity of each individual block. The spatial analysis was performed by dividing the area of study into 100 x 100 km^2 square cells with a 75% overlap, resulting in a final 25 x 25 km^2 pseudo-grid. For each cell containing at least 20 events, the lower seismicity cut-off was defined as the 90^{th} percentile of the frequency–depth distribution. In Figure 5 we displayed the results with a percentage error < 10%. As earthquakes occur in the brittle crust, this map can be interpreted as an instrumental evidence of the brittle-ductile transition. Although the brittle-ductile transition temperature suffers large uncertainties in the order of 475±175°C, a tiny seismogenic layer can be coexistent with a thermal anomaly and rise of deep crustal isotherms.

6. CONCLUSIONS

This study permitted to analyze in an integrated framework the temperature field in a wide region of the national territory. The main thermal anomalies locate in the Pliocene-Pleistocene volcanic districts where, locally, the 400°C isotherm results are shallower than 5 km. In these areas, several boreholes constrained the simulated thermal structure down to a depth of about 3 km with the highest measured temperature of 420°C in the San Vito well and 450°C in the Latera well located in the Campania and Roman Provinces, respectively. The zones where isotherms rise toward the Earth's surface display a shallow cut-off depth and essentially locate in a thinned/transitional crustal domain. Here, the seismogenic thickness of 8–10 km suggests high temperatures at the base of the regional hydrothermal reservoir are an important factor; this is also supported by the presence of thermal sources or geothermal manifestations. Large lateral rheological variations occur as a result of different tectonic processes leaving their signature especially in geothermal and crustal thickness. To this regard, the Tyrrhenian-Apennines system represents an outstanding example showing evidence of both extensional and compressional tectonic forces.

REFERENCES

Boccaletti, M., Calamita, F., Deiana, G., Gelati, R., Massari, F., Moratti, G., and Lucchi, F. R.: Migrating foredeep-thrust belt systems in the northern Apennines and southern Alps, *Palaeogeography, Palaeoclimatology, Palaeoecology*, **77**, (1990), 3-14.

Carminati, E., Doglioni, C., and Scrocca, D.: Alps vs Apennines, *Special volume of the Italian Geological Society for the IGC*, **32**, (2004), 141-151.

Cassano E., Fichera, R. and Arisi Rota, F.: Rilievo aeromagnetico d'Italia: alcuni risultati interpretativi, Atti del 5° Convegno Annuale del Gruppo Nazionale di Geofisica della Terra Solida, Roma 17 – 19 novembre 1986.

Castaldo R., G. Gola, A. Santilano, V. De Novellis, S. Pepe, M. Manzo, A. Manzella and P. Tizzani: The role of thermo-rheological properties of the crust beneath Ischia Island (Southern Italy) in the modulation of the ground deformation pattern, *Journal of Volcanology and Geothermal Research*, **344**, (2017), 154–173.

Chiarabba, C., and De Gori, P.: The seismogenic thickness in Italy: constraints on potential magnitude and seismic hazard, *Terra Nova*, **28**, (2016),402–408.

Cloetingh, S., van Wees, J.D., Ziegler, P.A., Lenkey, L., Beekman, F., Tesauro, M., Förster, A., Norden, B., Kaban, M., Hardebol, N., Bonté, D., Genter, A., Guillou-Frottier, L., Ter Voorde, M., Sokoutis, D., Willingshofer, E., Cornu, T., and Worum, G.: Lithosphere tectonics and thermo-mechanical properties: An integrated modelling approach for Enhanced Geothermal Systems exploration in Europe, *Earth-Science Reviews*, **102**, (2010), 159-206.

Della Vedova, B., Bellani, S., Pellis, G., and Squarci, P.: Deep temperatures and surface heat flow distribution. In: Vai, G.B., Martini, I.P. eds., Anatomy of an Orogen, The Apennines and Adjacent Mediterranean Basins, (2000). Kluwer Ac. Publ., Great Britain, 65-76.

Deming D.: Application of bottom-hole temperature corrections in geothermal studies, *Geothermics*, **18**, (1989), 775 – 786.

Dewey, J. F., Helman, M. L., Knott, S. D., Turco, E., & Hutton, D. H. W.: Kinematics of the western Mediterranean, *Geological Society, London, Special Publications*, **45**, (1989), 265-283.

Doglioni, C.: A proposal for the kinematic modelling of W-dipping subductions-possible applications to the Tyrrhenian-Apennines system, *Terra Nova*, **3**, (1991), 423-434.

Doglioni, C., Gueguen, E., Harabaglia, P., and Mongelli, F.: On the origin of west-directed subduction zones and applications to the western Mediterranean, *Geological Society, London, Special Publications*, **156**, (1999), 541-561.

Dowdle W.L. and W.M. Cobb: Static formation temperature from well logs - An empirical method. *Journal of Petroleum Technology*, **27**, (1975), 1326-1330.

ENEL/ENI–AGIP/CNR/ENEA: Inventario delle risorse geotermiche nazionali – Indagine d'insieme sul territorio nazionale. Ministero dell'industria, del commercio e dell'artigianato, (1988), 76 pages. Web site Italian Ministry of Economic Development. Last access 2 April 2019. https://unmig.mise.gov.it/index.php/it/dati/risorse-geotermiche/inventario-delle-risorse-geotermiche-nazionali.

ENEL/ENI-AGIP/CNR/ENEA: Inventario delle risorse geotermiche nazionali. Valutazione del potenziale geotermico nazionale. Aggiornamento 1994, 194 pp., 6 tav. Web site Italian Ministry of Economic Development. Last access 2 April 2018, https://unmig.mise.gov.it/index.php/it/dati/risorse-geotermiche/inventario-delle-risorse-geotermiche-nazionali.

Faccenna, C., Piromallo, C., Crespo-Blanc, A., Jolivet, L., and Rossetti, F.: Lateral slab deformation and the origin of the western Mediterranean arcs, *Tectonics*, **23**, (2004).

Horner D.R.: Pressure build-up in wells. *Proceeding the 3rd World Petroleum Congress*, 28 May-6 June, The Hague, the Netherlands, World Petroleum Congress (1951), pp. 25-43.

Ingebrigtsen, S.E., and Manning, C.E.: Implication of crustal permeability for fluid movement between terrestrial fluid reservoirs, *Journal of Geochemical Exploration*, **78**, (2003), 1-6.

Lavecchia, G., Boncio, P., Creati, N. and Brozzetti, F.: Some aspects of the Italian geology not fitting with a subduction scenario. *J. Virtual Explorer*, **10**, (2003), 1-14.

Liotta, D., Cernobori L. and Nicolich, R.: Restricted rifting and its coexistence with compressional structures: results from the Crop 03 traverse Northern Apennines, Italy, *Terra Nova*, **10**, (1998), 16-20.

Malinverno, A. and Ryan,W. B.: Extension in the Tyrrhenian Sea and shortening in the Apennines as result of arc migration driven by sinking of the lithosphere, *Tectonics*, **5**, (1986), 227-245.

Manning, C.E., and Ingebritsen, S.E.: Permeability of the continental crust: implications of geothermal data and metamorphic systems, *Review of Geophysics*, **37**, (1999), 127-150.

Mongelli, F., Zito, G., Della Vedova, B., Pellis, G., Squarci, P., and Taffi, L.: Geothermal regime of Italy and surrounding seas, In: V. Cermak and L. Rybach eds, Terrestrial Heat Flow and the Lithosphere Structure (1991), Springer-Verlag, Berlin Heidelberg, p. 507.

Montanari D., A. Minissale, M. Doveri, G. Gola, E. Trumpy, A. Santilano and A. Manzella: Geothermal resources within carbonate reservoirs in western Sicily (Italy): A review. *Earth-Science Reviews*, **169**, (2017), 180–201.

Montanari D., C. Albanese, R. Catalano, A. Contino, M. Fedi, G. Gola, M. Iorio, M. La Manna, S. Monteleone, E. Trumpy, V. Valenti and A. Manzella: Contour map of the top of the regional geothermal reservoir of Sicily (Italy), *Journal of Maps*, (2014).

Pasquale, V., Chiozzi, P., Gola, G. and Verdoya, M.: Depth–time correction of petroleum bottom-hole temperatures in the Po Plain, Italy, *Geophysics*, **73**, (2008), 187–196.

Pasquale, V., Gola, G., Chiozzi, P., and Verdoya, M.: Thermophysical properties of the Po Basin rocks, *Geophys. J. Int.*, **186**, (2011), 69-81.

Patacca, E. and Scandone, P.: The Plio-Pleistocene thrust belt-foredeep system in the southern Apennines and Sicily (Italy). *Geology of Italy*, *Special Volume of the Italian Geological Society for the IGC 32 Florence-2004*, 93-129.

Patacca, E., Sartori, R., and Scandone, P.: Tyrrhenian basin and Apenninic arcs: kinematic relations since Late Tortonian times. *Memorie della Società Geologica Italiana*, **45**, (1990), 425-451.

Peccerillo, A.: Plio-Quaternary Volcanism in Italy - Petrology, Geochemistry, Geodynamics, Springer-Verlag Berlin Heidelberg 2005.

Ranalli, G., and Rybach, L.: Heat flow, heat transfer and lithosphere rheology in geothermal areas: Features and examples, *Journal of Volcanology and Geothermal Research*, **148**, (2005), 3-19.

Royden, L., Patacca, E. and Scandone, P.: Segmentation and configuration of subducted lithosphere in Italy: an important control on thrust belt and foredeep-basin evolution, *Geology*, **15**, (1987), 714-717.

Scandone, P.: Origin of the Tyrrhenian Sea and Calabrian arc. *Bollettino della Società Geologica Italiana*, **98**, (1980), 27-34.

Scrocca, D., Carminati E., Doglioni C., Procaccianti D.: Tyrrhenian Sea, in Regional Geology and Tectonics: Phanerozoic Passive Margins, Cratonic Basins and Global Tectonic Maps, vol. 1C, edited by D. G. Roberts and A. W. Bally, (2012), 473-485, Elsevier, Amsterdam.

Trumpy, E., Manzella, A. Geothopica and the interactive analysis and visualization of the updated Italian National Geothermal Database. *Int. J. Appl. Earth Obs. Geoinf.*, **54**, (2017), 28-37.